FABRICATION OF SUPPORT-LESS ENGINEERED LATTICE STRUCTURES VIA JETTING OF MOLTEN ALUMINUM DROPLETS

Dinesh Krishna Kumar Jayabal*, Khushbu Zope*, and Denis Cormier*

*Department of Industrial and Systems Engineering, Rochester Institute of Technology, Rochester, NY 14623

Abstract

Magneto Hydro Dynamic (MHD) jetting is a promising new metal additive manufacturing technique that employs on-demand jetting of molten metal droplets onto a moving substrate. A particularly unique aspect of the process is its potential to print down-facing features without the need for support structures. Under suitable droplet jetting conditions affecting time and temperature, each droplet at least partially solidifies prior to impact of the next incoming molten metal droplet. The combination of droplet jetting frequency and substrate velocity dictates the step-over distance between incoming droplets. With relatively large droplet step-over distances (or equivalently small percentage of droplet overlap), it is possible to print unsupported down-facing features that are nearly parallel to the X-Y build platform. In this paper, we describe initial results in which engineered lattice structures have been printed using 4043 aluminum using this approach. A parametric study that maps jetting frequency and droplet step-over distance with the resulting lattice strut angle is presented. With careful control of jetting parameters, we show that it is possible to print nearly horizontal lines without any support.

Introduction

The majority of metal additive manufacturing research to date has focused primarily on powder bed fusion processes (e.g. DMLS, SLM, EBM, etc.), binder jetting of metals, or directed energy deposition. In all three of these process categories, the feedstock material used is typically metal powder. Powder-based processes are extremely versatile in the sense that most metals can readily be atomized into powder form. However, metal powders are typically much more expensive than the same alloy in wire or bar form, they require considerably more safety precautions than metal wire, and the high surface area-to-volume ratio makes them very susceptible to oxidation. Conversely, not all alloys can be easily drawn into wire form. The range of alloys available in wire form is therefore not as great as the range of alloys available in powdered form. Nevertheless, there has been a considerable growth of interest in wire-based metal additive manufacturing processes.

Examples of wire-based metal additive manufacturing include electron beam freeform fabrication (EBF^3) [1] and wire and arc additive manufacturing (WAAM) [2]. These processes feed wire into a melt puddle created by an electron beam or arc welding head. A new droplet jetting process that uses wire feedstock material is magneto hydro dynamic (MHD) liquid metal droplet jetting [3]. The MHD process melts wire in a micro crucible. The molten metal is directed into a pump chamber surrounded by a coil that induces eddy currents in the molten metal. Lorenz forces induce jetting of droplets at a specified frequency from the nozzle.

This paper is focused on the use of MHD droplet jetting to produce engineered lattice structures. With traditional powder bed fusion techniques, downward-facing surfaces of lattice struts are supported by unfused powder which is then removed after part fabrication. This generally works just fine if the lattice unit cell size is sufficiently large. Powder removal from lattice structures with small unit cell sizes can be a challenge though. Likewise, there is typically a desire to have components with completely solid skins. In powder bed fusion, a solid-skinned part with an engineered lattice core cannot be produced because there would be no way to remove unfused powder. In this paper, initial results are presented on research in which the MHD liquid metal jetting process developed by Vader Systems is used to fabricate engineered lattice structures without any support structures.

Experimental Setup

For this study, a Vader Systems MK1 drop-on-demand metal AM machine was used. The MK1 is based on the aforementioned magnetohydrodynamic jetting process. The printer setup consists of a spool of solid metal wire (4043 Al in this case) which is fed into a resistively heated chamber where it melts. A coil for electromagnetic pulsing results in Lorenz forces that cause ejection of discrete droplets from a ceramic nozzle. A level sensing laser system maintains a constant level of molten metal in the reservoir, and a thermocouple provides temperature control. As metals form oxides at elevated temperatures, a constant stream of argon is used to form an inert gas sheath around the jet. The components of the print head are shown in Figure 1.

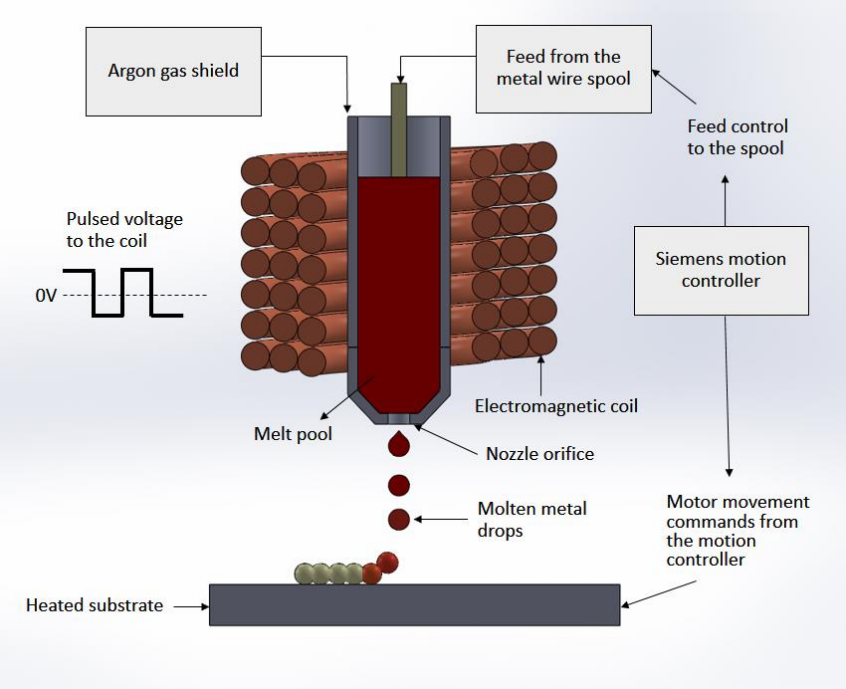

Figure 1: Vader MK1 print head components

With the MHD process, molten metal droplets are ejected through the nozzle by creating a pressure pulse within the molten metal pool inside the reservoir with help of a pulsed electromagnetic field. The pulsed field induces a transient current in the pool and as this induced current is under the applied field, the resulting Lorentz force causes the ejection of molten metal

droplets from the reservoir through the nozzle orifice. The characteristics of the pulsed field in question is dependent upon the input voltage and the waveform produced by the function generator. The frequency of the droplets ejected is controlled by the pulsing frequency of the coil. In the Vader Systems MK1 machine, the print head assembly moves up/down in the Z-axis direction, while the print bed moves in the X-Y plane. The timing of droplet ejection is coordinated with motion in the X, Y and/or Z-axis directions in order to build the desired 3D object. The process parameters that were held constant for the experiments in this research are provided in Table 1.

Table 1: Process parameters for the experiment.

Parameter	Value
Reservoir temperature (°C)	950
Print bed temperature (°C)	350
Argon flow rate (SCFH)	15
Nozzle diameter (µm)	500

By design, the Vader MK1 machine generates drops only when there is a movement in the Cartesian space. By choosing a value for drop spacing, one can instruct the machine to generate a drop every time it moves a distance matching the value set for the drop spacing. Here, the drop spacing is expressed through a drop overlap fraction for a given drop size as shown in the equation below.

$$Drop\ spacing = Drop\ diameter\ \times (1 - Drop\ overlap\ fraction) \quad \text{Equation 1}$$

Dropwise solidification occurs when droplets are deposited at a frequency low enough for one droplet to solidify before the next droplet arrives. If a newly arriving droplet's position is offset some amount relative to the last droplet, then an inclined column will form as droplets stack up. The degree of droplet overlap will affect the angle of the printed column. Likewise, the droplet jetting frequency will affect droplet solidification and spreading behavior. At higher frequencies, the columns tend to get shorter as a result of higher heat content and a greater degree of droplet spreading [4]. It is also to be noted that even though the nozzle diameter used in this research was 500 µm, the actual droplet size tends to be slightly smaller than this. As the strategy for building lattice structures is entirely dependent on the drop size, it is essential to measure drop size as a function of jetting parameters.

Parameter Mapping

For the droplet deposition experiment to print slanted pillars, factors such as droplet temperature, substrate temperature, droplet jetting frequency, stand-off distance between the print head and the substrate, and the droplet overlap fraction (which is the percentage fraction of the overlap between the two successive droplets (Equation 1) were considered. To understand the effect of these factors on the angles of the printed pillars, a full factorial study was performed. The factors and levels considered for this study are listed in Table 2.

Pillars printed at different process parameter settings are depicted in Figure 2. Each of the nine images depicts a set of pillars printed with droplet overlap fractions ranging from 0.5 to 1.

With a droplet overlap fraction of 1 (i.e. droplets overlap completely), a vertical pillar is formed at a 90° angle with respect to the substrate. As the overlap fraction decreases (i.e. there is less overlap between droplets), the angle of the pillar with respect to the substrate decreases.

Table 2: List of factors and levels used for the parameters mapping experiment

Factor	Levels
Stand-off distance (mm)	45, 65, and 85
Frequency (Hz)	9, 12, 15, 18, 21, 24, 27, and 30
Droplet overlap fraction	0.5 to 1 in steps of 0.025 (21 levels in total)

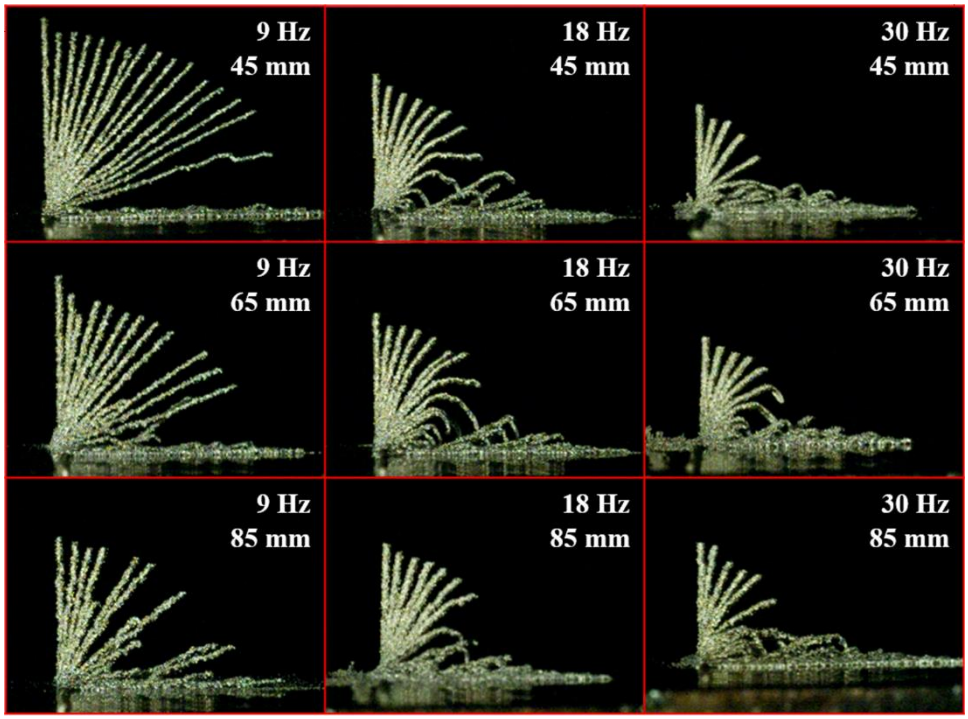

Figure 2: Printed pillars under different process parameters

As droplet jetting frequency was increased, the temperature increases, and droplet spreading increases. This generally results in shorter pillars with a larger diameter. However, with increased frequency, smaller droplet-overlap-fractions did not yield the linear slanted pillars but yielded wavy non-uniform pillars (Figure 3). At higher nozzle stand-off distance, more deformities were observed in the slanted pillars. The slanted pillars printed at every combination of frequency and stand-off distance were captured in images. These images were used to determine the angles between the slanted pillars and the substrate using ImageJ [5].

Collected data was plotted against frequency and droplet overlap fraction (Figure 4). Compared to stand-off distances of 45 and 85 mm, a 65 mm stand-off distance yielded more standing pillars. This can be explained on the basis of optimum pillar forming conditions. Good mechanical bonding between the two successive droplets can be achieved if the incoming droplet carries the sufficient thermal energy to re-melt the top surface of the previously deposited droplet. If this incoming thermal energy per unit time with the droplets is too low, as could happen in the case of low jetting frequency or/and higher stand-off distance, then either inter-droplet bonding will be weak or there will be no bonding at all. On the other hand, if the incoming thermal energy per unit time with the droplets is too high (e.g., high frequency or/and lower stand-off distance), then one deposited droplet has insufficient time to begin solidifying before the next droplet lands. In this case, the pillar slumps or does not form at all. Thus, to produce linear slanted pillars at a desired angle for a given engineered lattice structure, the droplets carrying the correct amount of thermal energy will result in an appropriate amount of remelting at the overlapping top surface of previously deposited droplets. As droplet overlap fraction increases, the angle formed with the substrate increases. A large set of parameter combinations at 65 mm stand-off distance resulted in suitable thermal energy for bonding and thus was used in subsequent experiments to print complete lattice structures.

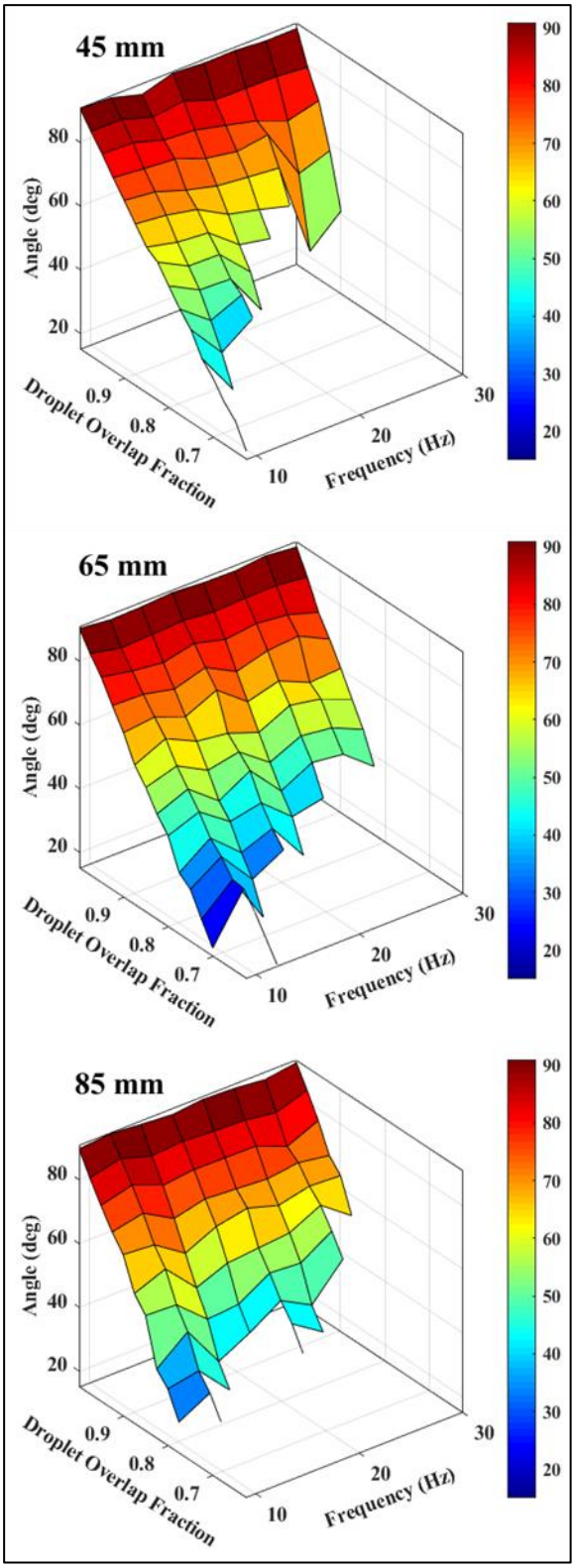

Figure 3: Correlation map between the frequency, droplet overlap fraction, and the angle formed by pillar with the substrate at three different stand-off distances.

Printing Lattice Structures

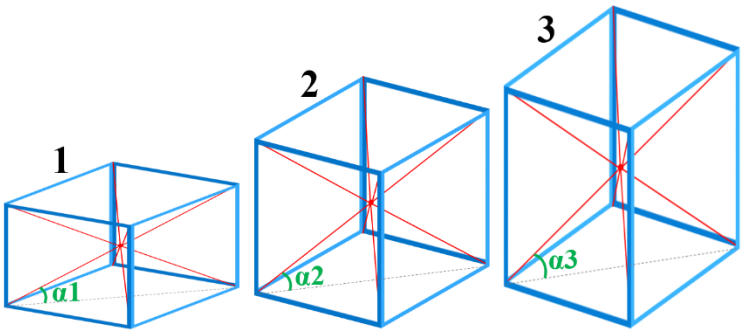

Figure 4: Cuboid geometries of the lattice unit cells with square shaped base area (w x w) and cell height (h), where α is the angle made by the slanted pillar with the bottom surface of the cuboid and α1 < α2 < α3.

Based on the knowledge obtained from the parameters mapping experiment, three different cuboid lattice unit cells were selected for the printing experiment (Figure 4 and Table 3). The printed lattices corresponding to parameter listed in Table 3 are shown in Figure 5. Angles mentioned in Table 3, were calculated from the dimensions of the lattice structures depicted in Figure 5.

Table 3: Printing parameters and geometrical dimensions of the lattice structures

Dimension or Parameter	Unit Cell 1	Unit Cell 2	Unit Cell 3
Unit Cell Width, *w* (mm)	5.3	6.1	6
Unit Cell Height, *h* (mm)	2.9	6.3	8.7
Diagonal Strut Angle, α (°)	21.15	36.14	45.71
Frequency (Hz)	12	21	27
Stand-off distance (mm)	65	65	65
Droplet overlap fraction	0.65	0.8	0.8
Droplet mass (µg)	105	148	126
Droplet diameter (µm)	420	472	447

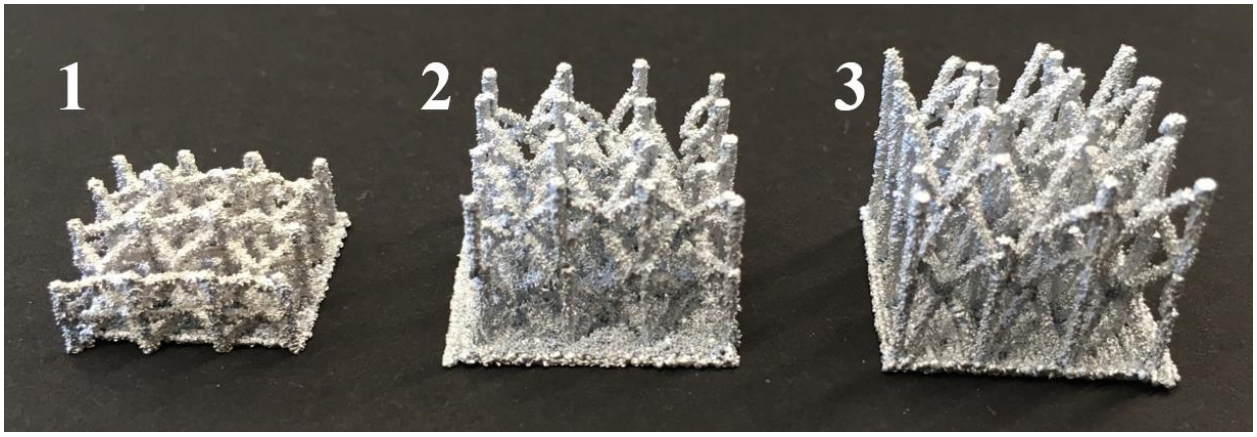

Figure 5: Lattice structures (3X3X2) with unit cells 1, 2, and 3. The printing parameters for these lattice structures were same as that for unit cells 1, 2, and 3, respectively.

A program was written to generate the G-code for printing lattice structures having the desired configurations and cell geometries. A subroutine in the program was written to print inclined pillars in the coordinates dictated by the unit cell geometry and the number of unit cells in the lattice structure. The generated G-code file is automatically converted to a file with an .mpf extension, the type which Vader MK1 uses for printing parts.

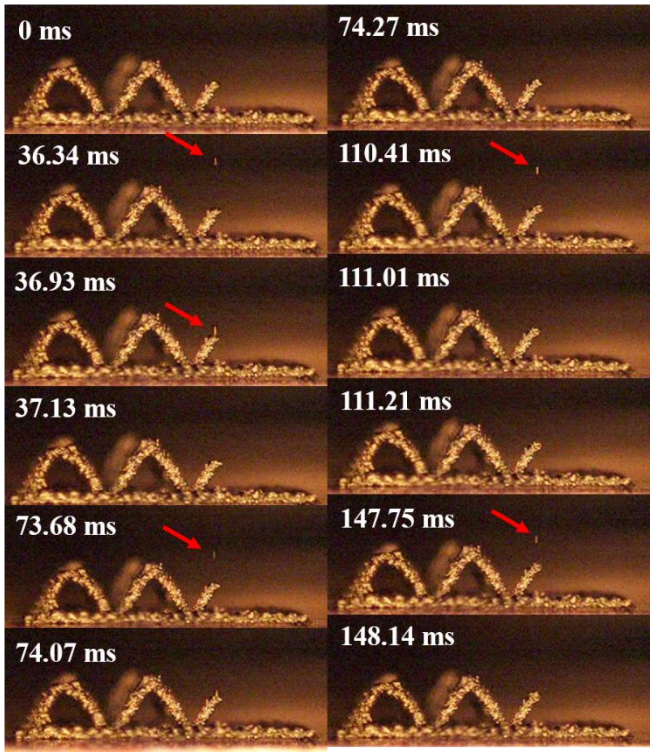

Figure 6: Frame by frame study of four droplet deposition. Droplet frequency = 27 Hz.

Stand-off distance was held constant at 65 mm for all three lattice prints. The droplet overlap fraction used in the unit cell 1 sample was smaller than that used for the unit cell 2 and 3 samples in order to produce a shallower strut angle. Likewise, the unit cell 1 sample was printed with a lower drop jetting frequency in order to reduce sagging, or drooping, of pillars due to the more shallow strut angle. The unit cell 2 and 3 samples were printed at same droplet overlap fraction with slight modification in the frequency. This was possible because of the different droplet masses. The droplet mass, and thus the droplet diameter, for the unit cell 2 sample was higher than that for the unit cell 3 sample. Larger diameter droplets carry higher thermal energy towards the pillar being printed and spread more than a comparatively smaller and lighter droplets. Thus, bigger droplets will facilitate more spreading of the droplets in the same linear length of the pillar. In the unit cell 2 sample, more packing of droplets resulted in shorter pillars and shallower angled pillars than that what was seen in the unit cell 3 samples.

The lattice structures were printed at the frequencies specified in Table 3. The printing of the slanted pillars was captured in high speed video using an Edgertronic SC2+ video camera at a frame rate of 5000 frames per second. These videos were studied to understand the landing and deformation of the droplets while printing (Figure 6). From the frame by frame image study, it appeared that the droplets were spreading to attain thin disk like shapes. In some cases, droplet oscillations after the deposition were also observed.

Conclusions

A set of experiments was conducted in order to assess the feasibility of producing engineered lattice structures without the need for support structures using drop-on-demand magnetohydrodynamic liquid metal droplet jetting. It was found that a droplet jetting frequency ranging from 12-27 Hz was able to produce mechanically sound inclined struts used in the lattice

structures. A droplet overlap fraction ranging from 0.5 to 1 produced struts of varying incline angles with respect to the substrate.

The ultimate aim of this research is to produce solid-skinned mechanical components with internal engineered lattice structures. Ongoing research with this technique is being conducted to print struts having arbitrarily large strut diameters. Mechanical properties of the lattice structures are also being studied. In the future, solid-skinned parts with embedded lattice structures will be printed.

References

[1] Gockel, J., Beuth, J. and Taminger, K., 2014. Integrated control of solidification microstructure and melt pool dimensions in electron beam wire feed additive manufacturing of Ti-6Al-4V. *Additive Manufacturing*, *1*, pp.119-126.

[2] Gu, J., Cong, B., Ding, J., Williams, S.W. and Zhai, Y., 2014, August. Wire+ arc additive manufacturing of aluminium. In *Proceedings of the 25th Annual International Solid Freeform Fabrication Symposium, Austin, TX, USA* (pp. 4-6).

[3] Sukhotskiy, V., Karampelas, H., Garg, G., Verma, A., Tong, M., Vader, S., Vader, Z., and Furlani, E. P., 2017, "Magnetohydrodynamic Drop-on-Demand Liquid Metal 3d Printing," Proceedings of the 28th Annual International Solid Freeform Fabrication Symposium, Austin, Texas., pp. 1806-1811.

[4] Gao, F. Q., and Sonin, A. A., 1994, "Precise Deposition of Molten Microdrops - the Physics of Digital Microfabrication," Proceedings of the Royal Society of London Series a-Mathematical Physical and Engineering Sciences, 444(1922), pp. 533-554.

[5] Ferreira, T., and Rasband, W., 2010-2012, Imagej User Guide — Ij 1.46, imagej.nih.gov/ij/docs/guide/.